iTRAQ-Based quantitative proteome revealed metabolic changes between a cleistogamous wheat mutant and its wild-type wheat

Caiguo Tang [1,2,†], Huilan Zhang [1,2,†], Pingping Zhang [3], Yuhan Ma [1], Minghui Cao [1,2], Hao Hu [1,2], Faheem Afzal Shah [1], Weiwei Zhao [1], Minghao Li [1,2,*] and Lifang Wu [1,*]

[1] Key laboratory of high magnetic field and Ion beam physical biology, Hefei Institutes of Physical Science, Chinese Academy of Sciences, Hefei 230031, Anhui, P.R. China;

[2] School of Life Sciences, University of Science and Technology of China, Hefei 230027, Anhui, P.R. China

[3] School of Life Sciences, Anhui University, Hefei 230601, Anhui, P.R. China

[†] These authors contributed equally to this work.

*Corresponding Author:

Minghao Li; Lifang Wu

350 Shushanhu Road, Hefei 230031, Anhui, P. R. China

Email address: limh@ipp.ac.cn (M.L); lfwu@ipp.ac.cn (L.W)

Abstract

Background: Wheat is one of the most important staple crops worldwide. However, *Fusarium* head blight severely affects wheat yield and quality. A novel bread wheat mutant, *ZK001*, characterized as cleistogamic was isolated from a non-cleistogamous varieties (YM18) through static magnetic fields mutagenesis. Cleistogamy should be a new strategy and approach to control *Fusarium* head blight. However, little is known about the mechanism of cleistogamy in wheat.

Methods: *Fusarium* head blight resistance test was performed to identify the *Fusarium* head blight infection rate of *ZK001*. And we measured the agronomic trait of *ZK001* and the contents of starch and total soluble sugar of lodicules in YM18 and *ZK001*. In addition, Comparative studies at the proteome level were employed between YM18 and *ZK001* based on the proteomic technique of isobaric tags for relative and absolute quantification.

Results: The infection rate of *ZK001* is lower than its wild type and AK58. The abnormal lodicules of *ZK001* lost the ability to push the lemma and palea apart during the flowering stage. Proteome analysis showed that the main differentially abundant proteins were related to carbohydrate metabolism, protein transport and calcium ion binding. These differentially abundant proteins may work together to regulate cellular homeostasis, osmotic pressure and the development of lodicules. This theory is supported by the analysis of starch, soluble sugar content in the lodicules as well as the results of qRT-PCR.

40 **Conclusions:** In this paper, we demonstrate that the proteome analysis provides comprehensive
41 information for further research on the lodicule development mechanism in wheat. This mutant is
42 optimal for studying flower development in wheat and could be very important for *Fusarium*
43 head blight resistant projects via conventional crossing.

44 **Key words:** Bread wheat, Cleistogamous, *Fusarium* head blight, Lodicule, iTRAQ

45

Introduction

47 Bread wheat (*Triticum aestivum* L.) is one of the most important staple crops worldwide. The
48 world population continues to grow and arable area is decreasing year by year, therefore higher
49 production in crop plants may prove to be necessary to satisfy the increasing demand in food
50 (FAO, 2015). However, many challenges like biotic and abiotic stress severely affect wheat
51 fields and the product quality. For instance, *Fusarium* head blight (FHB) is a critical factor badly
52 damaging wheat security (Walter, Nicholson & Doohan, 2010), and the application of chemical
53 insecticides and fungicides used for controlling pests and diseases is increasing the amount of
54 residues in wheat and in the environment (Hollingsworth et al., 2008). Therefore, scientists and
55 breeders have to find eco-friendly and cost-effective strategies to guarantee wheat yield and
56 quality. Induced mutation, such as Cobalt-60 (^{60}Co-γ-ray)-mutagenesis, static magnetic fields
57 (SMFs)-mutagenesis, spaceflight-mutagenesis, and ethyl methane sulfonate (EMS), is an
58 important method employed for crop breeding improvement (Krasileva et al., 2017).

59   In the last decade, severe epidemics caused by *Fusarium* ssp. have occurred worldwide and
60 up to 100% yield loss was recorded under optimal disease conditions (Yumurtaci et al., 2017).
61 FHB is a complex disease and the *pore-forming toxin-like* (*PFT*) gene at the quantitative trait
62 locus (QTL) *Fhb1* which so far was the first FHB-resistance gene was isolated and found to
63 confer resistance to FHB in Sumai 3 (SM3) (Rawat et al., 2016). FHB infection usually occurs
64 on the inner surfaces of lemmas and paleaes after germination of the *Fusarium* ssp. conidia
65 (Zange, Kang & Buchenauer, 2005). The anther can provide the initial path for FHB infection
66 (Pugh, Johann & Dickson, 1933; Walter, Nicholson & Doohan, 2010); therefore, cleistogamous
67 cultivars, which contain few anthers exposed to glumes, may provide structural barriers for
68 diseases that appear during the flowering stage. In barley (*Hordeum vulgare* L.), cleistogamous
69 cultivars, which self-fertilize within permanently closed flowers (Culley & Klooster, 2007),
70 showed greater resistance to FHB infection than chasmogamous cultivars, which have open
71 flowers (Yoshida, Kawada & Tohnooka, 2005). In wheat, cleistogamous cultivars (U24) have a
72 lower risk of FHB infection than chasmogamous cultivars such as Saikai 165 (Kubo et al., 2010).
73 Therefore, cleistogamy is a new strategy for controlling *Fusarium* head blight. Cleistogamy in
74 barley is genetically determined by the presence of the recessive allele *cly1*, but the dominant
75 allele at the linked locus, *Cly2*, is epistatic over *cly1* (Wang et al., 2013). Loss of the miRNA172
76 target site causes *cly1* to express a protein, HvAP2, which effectively suppress lodicule swelling
77 (Turuspekov et al., 2004; Nair et al., 2010; Wang et al., 2015). In rice, there are many
78 cleistogamous mutants resulting from abnormal lodicules. *ld(t)* (*lodiculeless spikelet(t)*), a single
79 recessive gene, controls the cleistogamous mutant lacking lodicules (Won & Koh, 1998; Maeng

80 et al., 2006). Another rice mutant, which has a truncated DEP2 determined by the *cl7(t)* gene,
81 has a cleistogamous phenotype because of weak swelling ability in the lodicules (Ni et al., 2014).
82 A third rice mutant, spw1-cls, has normal stamens, but the lodicules are transformed
83 homeotically into lodicule-glume mosaic organs, thereby engendering cleistogamy with
84 temperature-sensitivity (Yoshida et al., 2007; Ohmori et al., 2012). A novel temperature-stable
85 cleistogamous mutant, *spw1-cls2*, can maintain the cleistogamous phenotype under low
86 temperatures (Lombardo et al., 2017). The glumes open in the flowering stage because the
87 swelling of the lodicule is primarily responsible for pushing the lemma and palea, thereby
88 opening the floret (Nair et al., 2010). However, there is very little information on cleistogamy in
89 wheat.

90   The probability of primary infection is approximately proportional to the number of spores
91 reaching the open florets during the flowering process, and the breeding of varieties of flower
92 that are partially or completely cleistogamous might reduce *Fusarium* susceptibility in wheat
93 (Schuster & Ellner, 2008). In order to probe the mechanism of cleistogamy, Ning et al. (Ning et
94 al., 2013) studied the structure, transcription and post-transcriptional regulation of the
95 cleistogamous gene, *TaAP2*, which is homologous to barley in wheat. *TaAP2* alleles may also
96 generate a cleistogamous wheat and improve the resistance to FHB. Additionally, anther
97 extrusion is a complex trait with significant markers which has either favorable or unfavorable
98 additive effects and impart minor to moderate levels of phenotypic variance in spring and winter
99 wheat (Muqaddasi et al., 2017). Okada et al. (Okada et al., 2018) proposed a novel mechanism
100 where ovary swelling could push the lemma and palea apart to open the florets in wheat flowers.

101   Large-scale transcriptomic analyses have been employed in wheat to better understand the
102 molecular mechanisms of flower development (Winfield et al., 2010; Diallo et al., 2014; Feng et
103 al., 2015; Kumar et al., 2015; Yang et al., 2015; Ma et al., 2017). However, because of post-
104 transcriptional and post-translational modifications, the mRNA levels do not always correlate
105 with the corresponding protein levels (Schweppe et al., 2003; Canovas et al., 2004; Zhao et al.,
106 2013). Proteins are directly correlated with cellular functions (Yan et al., 2005; Zhang et al.,
107 2012); therefore, proteomic analysis is essential for studying global protein expression levels in
108 wheat to further unravel the complex mechanisms of cleistogamy. In particular, isobaric tags for
109 relative and absolute quantitation (iTRAQ) technology, which is a quantitative gel-free
110 proteomic approach, coupled with liquid chromatography/mass spectrometry/mass spectrometry
111 (LC/MS/MS) enables the direct quantification and comparison of protein levels among samples
112 with more efficiency and accuracy than traditional gel-based techniques which fail to identify
113 low-abundance protein species and have difficulties identifying proteins with extreme
114 biochemical properties (Wu et al., 2006).

115   Here, we show that an SMFs-induced wheat mutant, *ZK001*, is a cleistogamous line with
116 lower FHB infection vulnerability than the chasmogamous line, Yumai 18 (YM18).
117 Additionally, we perform a comparative proteomic analysis of different development stages in
118 YM18 and *ZK001* at Bangfei Bioscience (Beijing Bangfei Bioscience Co., Ltd.
119 http://www.bangfeibio.com/) to characterize the protein expression profiles. In the present study,

120 we attempted to provide insight into proteomic changes associated with the cleistogamous
121 phenotype in wheat, specifically exploring lodicule expanding mechanisms at the protein level.
122 The results have the potential to benefit future research efforts in controlling FHB via
123 conventional crossing and studying wheat flower development. It could also be important for
124 better control of genetically modified lines of agriculturally important crops; and it has time-
125 saving and cost-saving benefits in the purification of genotypes.

126 **Materials & Methods**

127 **Plant Material**

128 The cleistogamy mutant line, *ZK001*, was isolated from a mutagenized population of wheat
129 varieties, YM18, using SMFs with 7 Tesla for 5 hours. And it propagated via self-pollination
130 until the cleistogamous phenotype was completely stable. All wheat seeds were stored in Hefei
131 Institutes of Physical Science, Chinese Academy of Sciences (CASHIPS), Anhui, P. R. China.
132 Sumai 3 (SM3), Aikang 58 (AK58), YM18 and *ZK001* were grown in a greenhouse in an
133 experimental field (31°54′ N, 117°10′ E) at CASHIPS. Fertilizer and weed management were
134 similar to the process for wheat breeding (Li et al., 2014). The spikelets and lodicules of YM18
135 and *ZK001* which had three biological replicates were harvested during the white anther stage
136 (WAS), green anther stage (GAS), yellow anther stage (YAS) and anthesis stage (AS),
137 respectively (Zadoks, Chang & Konzak, 1974; Kirby & Appleyard, 1987; Guo & Schnurbusch,
138 2015). These samples were collected and frozen in liquid nitrogen and preserved at -80 °C.

139 **Starch and total soluble sugar content**

140 Twenty pairs of lodicules with three biological replications from YM18 and *ZK001* were
141 sampled and snap frozen in liquid nitrogen at four flower development stages. The samples were
142 grinded using Tissuelyser-24 (Shanghai Jingxin Industrial Development Co., Ltd.) for 45
143 seconds at 50 Hz.

144 Starch and total soluble sugars were extracted following the instructions included with the Starch
145 content kit and Plant soluble sugar content test kit (Nanjing Jiancheng Bioengineering Institute),
146 respectively. The starch and total soluble sugars in the supernatant were determined using a UV-
147 VIS Spectrophotometer (Lambda 365, PerkinElmer) with a wave length of 620 nm. The formula
148 of calculating starch and total soluble sugars as follow:

149

150 $$\text{Starch content} \left(\frac{\text{mg}}{\text{g}}\right) = \frac{\text{OD}_{\text{sample}} - \text{OD}_{\text{blank}}}{\text{OD}_{\text{standard}} - \text{OD}_{\text{blank}}} \times \text{Standard solution concentration} \left(0.2\frac{\text{mg}}{\text{ml}}\right) \times \text{V}_{\text{pretreatment solution}}$$
151 $$(\text{ml}) \times \text{Dilution ratio} \div \text{ of sample (g)}$$

152

153 $$\text{Total souble suger content (µg/g)}$$
$$= \frac{\text{OD}_{\text{sample}} - \text{OD}_{\text{blank}}}{\text{OD}_{\text{standard}} - \text{OD}_{\text{blank}}} \times \text{Standard solution concentration} \left(100\frac{\text{µg}}{\text{ml}}\right) \div \frac{\text{Weight of sample (g)}}{10 \times \text{V}_{\text{distilled water used for homogenating}}(\text{ml})}$$
$$\times \text{Dilution ratio}$$

154

155 **Observation of spikes and lodicules**

156 Spike images of YM18 and *ZK001* were captured with a camera (Nikon) at the AS. After 90
157 minutes, the lodicules of YM18 and *ZK001*, which were separated from the central young spikes

158 in triplicate during GAS and cultured on Murashige and Skoog (MS) medium, were observed
159 with an upright fluorescence stereomicroscope (Olympus) and captured by a camera (Olympus).

160 **FHB resistance testing**
161 FHB resistance testing was performed during the flowering stage of SM3, AK58, YM18 and
162 *ZK001* in the greenhouse by spraying the FHB spore F0601 (*Fusarium graminearum* Schw. cv.
163 F0601) in both 2013-2014 and 2014-2015. The inoculum (50 μL at 105 spores per mL) was
164 deposited by spraying on both sides of the ears. AK58 and SM3 were used as the susceptible and
165 resistant controls, respectively. The diseased spikelet rate was calculated using the following
166 formula: infected spikelets/total number of spikelets×100.

167 **Protein extraction and iTRAQ labelling**
168 Total soluble proteins were extracted according to a published procedure (Yang et al., 2013) with
169 slight modifications. Protein concentrations of the samples were estimated using the Bradford
170 method (Bradford, 1976) (Table S1) and the samples were stored at -80 °C for further use. All
171 protein samples were checked via sodium dodecyl sulphate polyacrylamide gel electrophoresis
172 (SDS-PAGE) according to the Schägger protocol (Schägger, 2006). SDS-PAGE gels (Figure S1)
173 were stained with Coomassie Brilliant Blue (CBB) staining solution (Commassie Blue Fast
174 Staining Solution, Beijing Dingguo Changsheng Biotechnology Co., LTD) (Kang et al., 2002).

175   After determining the protein concentration, Trypsin (Promega, V5113) was used to digest
176 and incubate for 12-16 h at 37 °C. About 100 μg peptides of different samples were labelled with
177 iTRAQ based on the Unwin et al. protocol (Unwin, Griffiths & Whetton, 2010). The peptides of
178 different samples were labelled with iTRAQ reagents (isobaric tags 113, 114, 115, 116, 117, 118,
179 119 and 121 for group YM18-WAS, *ZK001*-WAS, YM18-GAS, *ZK001*-GAS, YM18-YAS,
180 *ZK001*-YAS, YM18-AS and *ZK001*-AS, respectively) according to the manufacturer's
181 instructions (Applied Biosystems).

182 **HPLC grading of C18 columns at high pH and LC-electrospray ionization-MS/MS analysis**
183 The lyophilized peptide mixture was reconstituted with 100 μL of solution A (2% acetonitrile
184 (ACN) and 20 mM ammonium formate, pH 10). Then, the samples were loaded onto a reverse-
185 phase column (C18 column, 1.9 μm 150 μm × 120 mm, Thermo Scientific) and eluted using a
186 step linear elution program (Table S2). The samples were collected every 1.5 min and
187 centrifuged at 14,000 × g for 5-90 min. The 60 fractions collected were dried and re-dissolved
188 with 5 μL 0.5% formic acid (FA). The collected fractions were finally combined into 10 pools
189 and centrifuged at 14, 000 × g for 10 min.

190   The reconstituted peptides were analysed with the Q-Exactive HF mass spectrometer
191 (Thermo Fisher Scientific) coupled with a nano high-performance liquid chromatography system
192 (1260 Infinity II, Agilent) using 320 degrees centigrade temperature conditions (Scheltema et al.,
193 2014). The peptides were loaded onto a C18-reversed phase column (C18 column, 3 μm 100 μm
194 × 200 mm, Thermo Scientific) and separated on an analytical column (xBridge peptide BEH 130
195 C18 column, Waters) using mobile phases A (0.1% FA/H2O) and B (0.08% FA, 80% ACN)
196 (Table S3). The HPLC effluent was directly electrosprayed into the mass spectrometer and
197 analysed based on pre-set parameters (Figure S2).

198 **Data analysis**
199 The raw mass data were processed for peptide identification using Proteome Discoverer 1.4 (ver.
200 1.4.0.288, Thermo Fisher Scientific) with specific parameters (Table S4) for searching the
201 Uniprot Triticum database. False discovery rate (FDR) ≤ 0.01 was estimated for protein
202 identification using a target-decoy search strategy (Elias & Gygi, 2007). The mass spectrometry
203 proteomics data have been deposited to the ProteomeXchange Consortium
204 (http://proteomecentral.proteomexchange.org) via the PRIDE partner repository (Vizcaino et al.,
205 2016) with the dataset identifier < PXD010188 >. Up-regulated and down-regulated proteins
206 were determined based on 1.5-fold-changes and peptides spectral mathes (PSMs) ≥ 2 (Sharma et
207 al., 2017) between *ZK001*-WAS vs YM18-WAS (Group 1), *ZK001*-GAS vs YM18-GAS (Group
208 2), *ZK001*-YAS vs YM18-YAS (Group 3), *ZK001*-AS vs YM18-AS (Group 4), YM18-WAS vs
209 YM18-GAS (Group 5), YM18-WAS vs YM18-YAS (Group 6), YM18-WAS vs YM18-AS
210 (Group 7), *ZK001*-WAS vs *ZK001*-GAS (Group 8), *ZK001*-WAS vs *ZK001*-YAS (Group 9), and
211 *ZK001*-WAS vs *ZK001*-AS (Group 10), respectively.
212   Protein annotation was conducted by a BLAST search against NCBI and Uniprot databases.
213 Protein function was classified based on the following databases: Gene Ontology
214 (http://www.geneontology.org/, GO), and Kyoto Encyclopedia of Genes and Genomes
215 (http://www.genome.jp/kegg/, KEGG). For analysis of DAPs, significant GO enrichment and
216 KEGG enrichment were defined as a corrected FDR with a p–value (Benjamini & Hochberg,
217 1995) less than 0.01. Proteins containing at least two peptides spectral matches (PSMs) per
218 protein and fold change ratios ≥ 1.5 or ≤ 0.67 were considered as more abundant or less abundant
219 proteins, respectively. In order to validate the DEP profile, the EnsemblPlants database
220 (http://plants.ensembl.org/index.html) was searched for corresponding DNA sequences. A total
221 of 10 DAPs, which were carbohydarte, calcium ion binding and transport, were selected for
222 qRT-PCR validation.
223 **Quantitative Real-time PCR validation**
224 Total RNA was isolated using a Plant RNA Kit (Omega, R6827) according to the manufacturer's
225 instructions. The quality of each RNA sample was checked on 1% agarose gels. Measurement of
226 the concentration of RNA samples was performed using the NanoDrop 2000 spectrophotometer
227 bioanalyzer (Thermo Fisher Scientific). cDNAs were synthesized using TransScript One-Step
228 gDNA Removal and cDNA Synthesis SuperMix (Transgen Biotech) according to the
229 manufacturer's protocol. qRT-PCR was used to measure the transcript levels of the proteins of
230 interest. Each experiments were performed in three technical replicates with three biological
231 replicates. Target gene-specific primers (Table S5) were designed using the online software
232 Primer 3 version 0.4.0 (http://bioinfo.ut.ee/primer3-0.4.0/primer3/) (Untergasser et al., 2012).
233 Quantitative reverse transcription polymerase chain reaction (qRT-PCR) was performed
234 according to the manufacturer's instructions for the FastStart Essential DNA Green Master
235 (Roche), run in the Roche LightCycler® 96 Instrument. The *glyceraldehyde-3-phosphate*
236 *dehydrogenase* gene from *T. aestivum* (*TaGAPDH*, GI: 7579063) was served as an internal

237 control and the relative expression of target genes was calculated using the $2^{-\Delta\Delta CT}$ method (Livak
238 & Schmittgen, 2001).

239 **Statistical data analysis**
240 The experimental data values represented the average of the measurements conducted from three
241 independent assays and were expressed as the mean ± standard error of the mean (SEM). The
242 data were further analyzed using an ANOVA at a 95% confidence level followed by Duncan's
243 test (SPSS 18.0, IBM, Somers, NY, USA). The level of significance was set at $p \leq 0.05$.

244

Results

246 **Comparison of resistance to *Fusarium* head blight**
247 Since the cleistogamous wheat mutant was isolated, we identified this cleistogamous mutant with
248 a low FHB infection comparing to chasmoigamous varieties. Kubo et al. (Kubo et al., 2010)
249 showed that cleistogamous wheat cultivars have a lower FHB infection rate than chasmogamous
250 cultivars. Therefore, we tested the FHB resistance of YM18 and *ZK001*. The results of FHB
251 resistance testing showed that the infection rate in Sumai 3 (SM3) and *ZK001* were 7.03% and
252 9.39% in 2013-2014 and 8.61% and 17.60% in 2014-2015, respectively (Table 1). Compared to
253 SM3 and *ZK001*, YM18 and Aikang (AK58) were highly susceptible, 35.16% and 38.12% in
254 2014-2015, respectively. However, the diseased spikelet rates for YM18 and AK58 were 15.20%
255 and 20.41% in 2013-2014, respectively, about half the rate in 2014-2015 (Table 1). It indicates
256 that the FHB infection rate is greatly influenced by environmental factors. These results
257 suggested that cleistogamous cultivars had a lower FHB infection rate than chasmoigamous
258 cultivars. In addition, this mutant should be capable of generating excellent varieties with the
259 phenotype of cleistogamy via conventional hybridization.

260

261 **Comparison of flower between YM18 and *ZK001***
262 Exserted anthers increased the incidence of FHB (Sage & De Isturiz, 1974; PARRY,
263 JENKINSON & McLEOD, 1995). Furthermore, the anthers of cleistogamy wheat were detained
264 in glums during the flowering stage. The individual lines of YM18 and *ZK001* were grown under
265 the same growth and environmental conditions but the morphological differences were obvious.
266 In YM18, the anthers extrude from the palea and lemma at the anthesis stage (AS), whereas no
267 anthers were observed in *ZK001* at all flower development stages (Figure 1A). The morphology
268 of the lodicules of YM18 and *ZK001* was also obviously different. In order to investigate the
269 morphology of the lodicules, the lodicules of YM18 and *ZK001* at the green anther stage (GAS)
270 were harvested and cultured for 90 minutes on MS medium. The results showed that the width of
271 YM18 lodicules (Figure 1B) was larger than that of *ZK001* lodicules (Figure 1C and 1D).

272

273 **Physiological characters of lodicules in YM18 and *ZK001***
274 To reveal the cause of the lodicules difference between YM18 and *ZK001*, the starch and total
275 soluble sugar contents were measured in the lodicules of YM18 and *ZK001* at four flower
276 development stages. Lodicule starch and total soluble sugar contents showed an overall increase

277 from white anther stage (WAS) to AS for YM18 and *ZK001* (Figure 2, Table S6). No significant
278 differences in the starch and soluble sugar contents in the lodicule were observed in YM18 or
279 *ZK001* during WAS and GAS. Additionally, the starch and total soluble sugar contents in *ZK001*
280 decreased by 2.54, 2.40, 2.30, and 1.75-fold compared with YM18 during the yellow anther
281 stage (YAS), detected in the quality fraction and per pair of lodicules, respectively (Figure 2,
282 Table S6). In contrast, the starch and total soluble sugar contents in *ZK001* increased by 4.50,
283 3.57, 1.87, and 1.52-fold compared with YM18 during the AS, detected in the quality fraction
284 and per pair of lodicules, respectively (Figure 2, Table S6).
285
286 **Overview of quantitative proteome analysis**
287 In order to study the protein expression patterns in YM18 and *ZK001*, the proteomes of YM18
288 and *ZK001* in the four flower development stages were examined and quantitatively catalogued
289 using iTRAQ technology, respectively. In this study, 19,422 peptides were matched to 4,497
290 proteins in the samples (Table S7); in addition, 11,603 unique peptides were found, and 2,172
291 proteins were identified with more than two unique peptide sequences excluding PTMs. Figure
292 3A shows that more than 99% of the peptides covered proteins within the 36 peptides, and
293 protein quantity decreased as the number of matching peptides increased. In terms of protein
294 mass distribution, good coverage (average of 10–18% of total proteins in each protein-mass
295 group) was obtained for proteins > 10 kDa and < 60 kDa (Figure 3B). The length of the
296 identified peptides was between 10 and 13 aas at the peak and about 93% of the peptide length
297 was within 24 aas (Figure 3C). Over 77% of the proteins had > 5% sequence coverage.
298 Additionally, sequence coverage distribution was high in most of identified proteins: more than
299 58% had over > 10% coverage and more than 37% had over 20% coverage (Figure 3D). These
300 results indicate that the identified peptides were sufficient for protein identification.
301
302 **Formatting of Mathematical Components**
303 In order to identify more differentially abundant proteins, we compared the differentially
304 abundant proteins between YM18 and *ZK001* in the flowering development process, *ZK001*-
305 WAS vs YM18-WAS (Group 1), *ZK001*-GAS vs YM18-GAS (Group 2), *ZK001*-YAS vs
306 YM18-YAS (Group 3), *ZK001*-AS vs YM18-AS (Group 4), YM18-WAS vs YM18-GAS (Group
307 5), YM18-WAS vs YM18-YAS (Group 6), YM18-WAS vs YM18-AS (Group 7), *ZK001*-WAS
308 vs *ZK001*-GAS (Group 8), *ZK001*-WAS vs *ZK001*-YAS (Group 9), and *ZK001*-WAS vs *ZK001*-
309 AS (Group 10), respectively. Increasing abundance and decreasing abundance proteins were
310 determined based on fold-changes (FC) of > 1.5 or < 0.667 for expression difference
311 comparison. For further screening, about 16, 47, 2, 0, 11, 124, 105, 15, 298 and 188 differentially
312 abundant proteins (DAPs) were identified with a corrected P–value for GO KEGG enrichment
313 less than 0.01 in group 1 to 10 (Table 2). A Venn diagram of the DAPs and their overlap
314 between Group 1 and Group 2 showed that 2 and 1 common DAPs were increased-abundance
315 and decreased- abundance, respectively (Figure S3). Group 3 and Group 4 showed no overlap

316 with Group 1 or Group 2 (Figure S3). Venn diagrams indicated that 6, 10, 32, 206, 57 and 140
317 DAPs were specific DAPs of Groups 5, 8, 6, 9, 7 and 10, respectively (Figure S3).
318   Furthermore, there were more DAPs during WAS (Group 1) / GAS (Group 2) than during
319 YAS (Group 3) and AS (Group 4). With the growth of the plant, the mass of DAPs continued
320 increasing from WAS to YAS in both YM18 and *ZK001* (Groups 5 to 6 and Groups 8 to 9,
321 respectively). However, there was a disparity between YM18 and *ZK001* from YAS to AS. The
322 number of DAPs decreased by about 39% in *ZK001* from YAS to AS (Group 10), but showed a
323 slight decrease in YM18 (Group 7) (Table 2).
324

325 **Functional classification and subcellular localization of proteins**
326 GO analysis showed that all of the identified proteins in YM18 and *ZK001* were involved in 11
327 subgroups of MF, 19 subgroups of BP, and 14 subgroups of CC (Figure S4). Significant GO
328 enrichment was employed to analyse the DAPs with a corrected FDR P–value less than 0.01, and
329 a ratio FC of more than 1.5. Based on GO annotations and enrichments, the DAPs of Group 1
330 were enriched in molecular function terms for lipid binding (100%) (Figure 4A), as well as
331 biological process terms for lipid transport (14.06%), lipid localization (14.06%), macromolecule
332 localization (20.31%), organic substance transport (20.31%), single-organism transport (15.63%)
333 and single-organism localization (15.63%) (Figure 4B). GO classification of Group 2 revealed
334 that the DAPs were enriched in the biological process, cellular component and molecular
335 function (Figure 4C). No protein was enriched in Group 3 or Group 4. The DAPs of Groups 5 to
336 10 were also classified into biological process (Figure S5A), cellular component (Figure S5B)
337 and molecular function (Figure S5C). DAPs involved in carbohydrate metabolism and transport,
338 calcium ion binding and protein transport, fatty acid biosynthesis and signal transduction-related
339 proteins were further used in cluster analyses.
340

341 **Accumulation patterns of DAPs and verification of DAPs interest**
342 Based on the above analyses, 11 genes which corresponded to DAPs of interest were chosen for
343 qRT-PCR analyses using gene-specific primers (Table S5) to explore the expression profile at
344 the transcription level.
345   The morphology of lodicules showed significant differences between YM18 and *ZK001*
346 (Figure 1). qRT-PCR was carried out using the RNA of YM18 and *ZK001* lodicules to study the
347 transcript profiles of the above genes corresponding to the selected DAPs (Figure 5). The results
348 of qRT-PCR indicated that the expression level of The gene of *A0A1D6CCI3* (bidirectional sugar
349 transporter SWEET) was expressed in the lodicules at WAS and GAS of both YM18 and ZK001,
350 while almost no expression at YAS and AS (Figure 3, Table S7); (Figure 5A). Additionally, the
351 expression trend of this gene revealed down-regulation from WAS to GAS and YAS, and then
352 up-regulation to the initial expression level during AS in *ZK001* (Figure 5A). Furthermore, the
353 expression trend in YM18 showed a certain similarity to that in *ZK001* (Figure 5A). The
354 expression level of the gene *A0A1D5WGA3* was extremely down-regulated from WAS to GAS
355 in YM18 and *ZK001*, respectively (Figure 5B). Though the relative expression level in *ZK001*

356   was higher than that in YM18, there were almost no significant differences between YM18 and
357   *ZK001* in GAS, YAS or AS (Figure 5B). Compared with the relative expression levels of the
358   gene encoding A0A1D5RR02 in YM18, the gene in *ZK001* was down-regulated during WAS
359   and GAS, respectively (Figure 5C). There was no significant difference during YAS or AS
360   (Figure 5C). Additionally, compared with YM18, P93594-encoding mRNA was all up-regulated
361   in the lodicules of *ZK001* (Figure 5D). Interestingly, the mRNA level of W5B5R3 in *ZK001*
362   indicated up-regulation compared with YM18 at YAS and AS, respectively, while there was no
363   significant difference during WAS or GAS (Figure 5E). The mRNA levels of *A0A1D5SYC3* and
364   *A0A1D5VEI9* showed almost no significant difference between YM18 and *ZK001* at the four
365   flower development stages, except that of A0A1D5SYC3 (Figure 5F) and A0A1D5VEI9 (Figure
366   5G). The relative expression level for *A0A1D5RVB4* was up-regulated in *ZK001* compared with
367   that in YM18 at GAS, YAS and AS (Figure 5H). Comparing with YM18, the gene expression of
368   A0A077S2F2 in *ZK001* was down-regulated during YAS (Figure 5I).
369   Calcium ion plays a key role in the development of plants. Therefore, the relative
370   expression of the genes encoding A0A1D5TN57 and A0A1D5RRV7 was also evaluated to
371   determine the profile during flower development. Compared with YM18, the relative gene
372   expression levels of A0A1D5TN57 in *ZK001* were up-regulated during WAS, YAS and AS,
373   respectively (Figure 5K), while those of A0A1D5RRV7 were up-regulated during WAS, GAS
374   and AS (Figure 5J).

Discussion

Cleistogamy provides structural barriers for diseases of *Fusarium* head blight

377   From the physiological point of view, the flowering stage is regarded as the most susceptible
378   period for primary infection of wheat spikes by FHB because of the opening of wheat florets and
379   the extension of anthers (Pugh, Johann & Dickson, 1933; Schroeder & Christensen, 1963;
380   Gilsinger et al., 2005; Schuster & Ellner, 2008). Barley is the plant that self-fertilizes with
381   permanently closed flowers, but it is easy to be infected with *Fusarium* in chasmogamous barley
382   varieties (Yoshida, Kawada & Tohnooka, 2005; Culley & Klooster, 2007). Table 1 shows that
383   the diseased spikelet rate in 2014-2015 was more severe than that in 2013-2014 except in SM3,
384   possibly because of the resistance gene *Fhb1* (Rawat et al., 2016). Compared with YM18, which
385   is a wild type and chasmogamous cultivar, the diseased spikelet rate for *ZK001*, which is a
386   mutant and cleistogamous cultivar, decreased by 38.22% and 50.00% in 2013-2014 and 2014-
387   2015, respectively (Table 1). This indicates that although the diseased spikelet rate is greatly
388   influenced by environmental factors, cleistogamous cultivars that flower partially or completely
389   may have a lower risk of FHB infection than chasmogamous cultivars (Kubo et al., 2010; Wang
390   et al., 2013). Therefore, we further verified the hypothesis that cleistogamous cultivars might
391   have lower *Fusarium* susceptibility in wheat. From the practical point of view, as a new strategy
392   for controlling FHB, it will be very meaningful to introduce the cleistogamous function into
393   other varieties that are suitable for production and promotion but sensitive to FHB through
394   hybridization.

Lodicules play an important role in glume opening/closing in wheat

396 The molecular mechanism for cleistogamy had been intensively studied in rice (Maeng et al.,
397 2006; Yoshida et al., 2007; Ohmori et al., 2012; Ni et al., 2014; Lombardo et al., 2017) and
398 barley (Turuspekov et al., 2004; Hori et al., 2005; Nair et al., 2010; Wang et al., 2013, 2015;
399 Zhang et al., 2016). However, the molecular mechanism for cleistogamy remains unclear beyond
400 the knowledge that lodicule is a key factor in glume opening/closing in the monocotyledon. The
401 abnormal lodicules may lack the ability to push the lemma and palea apart during the flowering
402 stage in the cleistogamous mutant *ZK001* (Figure 1). This phenomenon is similar to that in barley
403 (Nair et al., 2010).

404 **Carbohydrates and calcium are the main factors regulating lodicule osmotic pressure**
405 Sucrose is the primary form by which sugar is transported for photosynthetic carbon assimilation
406 (Chen et al., 2012). The gene of *A0A1D6CCI3* was expressed in the lodicules of both YM18 and
407 *ZK001* (Figure 5A, Table S8). This indicates that carbohydrates can be transferred to the
408 lodicules of both YM18 and *ZK001* normally. Nevertheless, the starch and soluble sugar content
409 in the lodicules of YM18 increased dramatically from GAS to YAS (Figure 2A-D, Table S6).
410 Liu et al. (Liu et al., 2017) suggested that retarded lodicule expansion in ZS97A was caused by
411 reduced water accumulation because of retarded accumulation of osmotic regulation substances.
412 In contrast, the lower soluble sugar content in the lodicules of *ZK001* prevented the accumulation
413 of water during YAS (Figure 2C and 2D, Table S6). The lodicule mass of YM18 was higher than
414 that of *ZK001* because the starch and soluble sugar contents in the lodicules of *ZK001* decreased
415 from GAS to YAS, leading to little water transfer to the lodicules. The lodicules of wheat swell
416 extensively and subsequently contract after rapid autolyzation of the tissues (Craig & O'Brien,
417 1975). Therefore, the starch and soluble sugar contents in the lodicule of YM18 were lower than
418 those in *ZK001* at AS (Figure 2A-D, Table S6).

419   Cytosolic calcium is an important secondary messenger in plants and plays important roles
420 in the response to both environmental and internal signals (Poovaiah & Reddy, 1993; Liao,
421 Zheng & Guo, 2017). Plant annexins are calcium-dependent phospholipid binding proteins with
422 many biological functions; for instance, they participate in calcium ion channel formation,
423 membrane dynamics, plant growth and the stress response (Mortimer et al., 2008; Laohavisit &
424 Davies, 2011). In this study, the gene relative expression levels of annexin (A0A1D5RRV7) and
425 the calcium ion binding-related protein (A0A1D5TN57) in the lodicules of *ZK001* were up-
426 regulated during WAS compared to those of YM18, respectively (Figure 5J and 5K). Therefore,
427 we inferred that WAS was a critical period for the lodicules.

428 **An overview of the pathways for proteome metabolic changes in lodicules**
429 Many factors regulate the osmotic pressure of lodicules, such as soluble sugar (Zee & O'Brien,
430 1971; Wang, Gu & Gao, 1991; Yan et al., 2017), starch (Pissarek, 1971), calcium (Qin, Yang &
431 Zhao, 2005; Chen et al., 2016) and potassium (Heslop-Harrison & Heslop-Harrison, 1996; Chen
432 et al., 2016; Liu et al., 2017). In this paper, we propose an overview of the metabolic pathways
433 involving the carbohydrates that regulate the osmotic pressure of the lodicules. Our results and
434 previous studies provide an overview of the osmotic mechanisms. As shown in Figure 6, sucrose
435 is transferred into the lodicules from the extra-cellular environment through a bidirectional sugar

436 transporter, and is converted into d-fructose-6p by hexokinase after being broken down into d-
437 fructose. d-fructose-6p converted to α-d-flucose-1p, which can be converted to d-flucose by β-
438 glucosidase and synthetized amylose. The starch formed by amylose can be broken down into d-
439 glucose under the action of β-amylase. UDP-glucose formed from amino sugar and nucleotide
440 sugar can also be converted into d-glucose under the action of β-glucosidase. The accumulation
441 of d-glucose leads to a change in osmotic pressure in the lodicules. Additionally, α-d-glucose-1p
442 can enter the pentose phosphate pathway and the fatty acid biosynthesis pathway through the
443 formation of α-d-glucose-6P and β-d-glucose-6P. Soluble sugar can also enter and exit cells
444 through the bidirectional sugar transporter. Furthermore, annexin can trigger calcium ion influx,
445 increasing the osmotic pressure. Once the osmotic pressure changes, water accumulates in / is
446 excreted from the cells of the lodicules and induces the expansion / shrinkage of the lodicules.
447

Conclusions

449 The wheat mutant, *ZK001*, with the atrophied, thin and ineffective lodicules lost the ability to
450 push the lemma and palea apart in the flower development process. Besides, compared with
451 YM18, *ZK001* showed lower *Fusarium* infection because of the cleistogamous phenotype.
452 Furthemore, we speculated that the thin lodicule of *ZK001* resulted from the lower soluble sugar,
453 calcium ion and potassium ion contents in lodicule which were regulated by carbohydrate
454 metabolic, protein transport, and calcium ion binding-related proteins. Though, little is known
455 about the mechanism of cleistogamy in wheat, we propose an overview metabolic pathway about
456 the carbohydrate which regulates the osmotic pressure of the lodicules. This study provides
457 foundations for researchers to explore the mechanism of cleistogamy. Furthermore, it should be
458 possible to generate a cleistogamous wheat via conventional crossing, which would improve the
459 FHB resistance of wheat and control pollen-mediated gene flow of genetically modified wheat.
460

Acknowledgements

462 We thank Xiue Wang, College of Agriculture, Nanjing Agricultural University, for providing
463 FHB spore F0601. We also thank Shiliang Li and Shengqun Zheng for field management. This
464 work was funded by the Science and Technology Service program of Chinese Academy of
465 Sciences (KFJ-STS-ZDTP-002), the key program of 13th five-year plan, CASHIPS (No. kp-
466 2017-21), the major special project of Anhui Province (16030701103). This study is also
467 supported by the Natural Science Foundation of Anhui Provincial (1408085QC64), the Opening
468 Fund of State Key Laboratory of Crop Genetics and Germplasm Enhancement (ZW2013003).

469

References

471 Benjamini Y, Hochberg Y. 1995. Controlling the False Discovery Rate - a Practical and
472   Powerful Approach to Multiple Testing. *Journal of the Royal Statistical Society Series B-*
473   *Methodological* 57:289–300.

474 Bradford MM. 1976. Rapid and sensitive method for quantitation of microgram quantities of
475   protein utilizing principle of protein-dye binding. *Analytical Biochemistry* 72:248–254.
476   DOI: 10.1006/abio.1976.9999.
477 Canovas FM, Dumas-Gaudot E, Recorbet G, Jorrin J, Mock HP, Rossignol M. 2004. Plant
478   proteome analysis. *Proteomics* 4:285–298. DOI: 10.1002/pmic.200300602.
479 Chen Y, Ma J, Miller AJ, Luo B, Wang M, Zhu Z, Ouwerkerk PB. 2016. OsCHX14 is Involved
480   in the K+ Homeostasis in Rice (Oryza sativa) Flowers. *Plant Cell Physiol* 57:1530–1543.
481   DOI: 10.1093/pcp/pcw088.
482 Chen LQ, Qu XQ, Hou BH, Sosso D, Osorio S, Fernie AR, Frommer WB. 2012. Sucrose Efflux
483   Mediated by SWEET Proteins as a Key Step for Phloem Transport. *Science* 335:207–211.
484   DOI: 10.1126/science.1213351.
485 Craig S, O'Brien TP. 1975. The Lodicules of Wheat: Pre- and Post-Anthesis. *Australian Journal*
486   *of Botany* 23:451–458. DOI: 10.1071/BT9750451.
487 Culley TM, Klooster MR. 2007. The cleistogamous breeding system: A review of its frequency,
488   evolution, and ecology in angiosperms. *Botanical Review* 73:1. DOI: 10.1663/0006-
489   8101(2007)73[1:TCBSAR]2.0.CO;2.
490 Diallo AO, Agharbaoui Z, Badawi MA, Ali-Benali MA, Moheb A, Houde M, Sarhan F. 2014.
491   Transcriptome analysis of an mvp mutant reveals important changes in global gene
492   expression and a role for methyl jasmonate in vernalization and flowering in wheat. *J Exp*
493   *Bot* 65:2271–2286. DOI: 10.1093/jxb/eru102.
494 Elias JE, Gygi SP. 2007. Target-decoy search strategy for increased confidence in large-scale
495   protein identifications by mass spectrometry. *Nat Methods* 4:207–214. DOI:
496   10.1038/nmeth1019.
497 FAO. 2015. *FAO statistical pocketbook, World food and agriculture 2015, Rome, Food and*
498   *Agricultural Organization of the United Nations*.
499 Feng YL, Wang KT, Ma C, Zhao YY, Yin J. 2015. Virus-induced gene silencing-based
500   functional verification of six genes associated with vernalization in wheat. *Biochem Biophys*
501   *Res Commun* 458:928–933. DOI: 10.1016/j.bbrc.2015.02.064.
502 Gilsinger J, Kong L, Shen X, Ohm H. 2005. DNA markers associated with low Fusarium head
503   blight incidence and narrow flower opening in wheat. *Theoretical and Applied Genetics*
504   110:1218–1225. DOI: 10.1007/s00122-005-1953-4.
505 Guo Z, Schnurbusch T. 2015. Variation of floret fertility in hexaploid wheat revealed by tiller
506   removal. *J Exp Bot* 66:5945–5958. DOI: 10.1093/jxb/erv303.
507 Heslop-Harrison Y, Heslop-Harrison JS. 1996. Lodicule Function and Filament Extension in the
508   Grasses: Potassium Ion Movement and Tissue Specialization. *Annals of Botany* 77:573–
509   582. DOI: 10.1006/anbo.1996.0072.
510 Hollingsworth CR, Motteberg CD, Wiersma J V, Atkinson LM. 2008. Agronomic and Economic
511   Responses of Spring Wheat to Management of Fusarium Head Blight. *Plant Disease*
512   92:1339–1348. DOI: 10.1094/PD1S-92-9-l339.
513 Hori K, Kobayashi T, Sato K, Takeda K. 2005. QTL analysis of Fusarium head blight resistance
514   using a high-density linkage map in barley. *Theor Appl Genet* 111:1661–1672. DOI:
515   10.1007/s00122-005-0102-4.
516 Kang DH, Gho YS, Suh MK, Kang CH. 2002. Highly sensitive and fast protein detection with
517   coomassie brilliant blue in sodium dodecyl sulfate-polyacrylamide gel electrophoresis.
518   *Bulletin of the Korean Chemical Society* 23:1511–1512. DOI:
519   10.5012/bkcs.2002.23.11.1511.

520 Kirby EJM, Appleyard M. 1987. *Cereal Development Guide*. 2nd ed Stoneleigh, UK: NAC
521   Cereal Unit, 85pp.
522 Krasileva K V, Vasquezgross HA, Howell T, Bailey P, Paraiso F, Clissold L, Simmonds J,
523   Ramirezgonzalez RH, Wang X, Borrill P. 2017. Uncovering hidden variation in polyploid
524   wheat. *Proc Natl Acad Sci U S A* 114:E913.
525 Kubo K, Kawada N, Fujita M, Hatta K, Oda S, Nakajima T. 2010. Effect of cleistogamy on
526   Fusarium head blight resistance in wheat. *Breed Sci* 60:405–411. DOI:
527   10.1270/jsbbs.60.405.
528 Kumar RR, Goswami S, Sharma SK, Kala YK, Rai GK, Mishra DC, Grover M, Singh GP,
529   Pathak H, Rai A, Chinnusamy V, Rai RD. 2015. Harnessing Next Generation Sequencing in
530   Climate Change: RNA-Seq Analysis of Heat Stress-Responsive Genes in Wheat (Triticum
531   aestivum L.). *OMICS* 19:632–647. DOI: 10.1089/omi.2015.0097.
532 Laohavisit A, Davies JM. 2011. Annexins. *New Phytologist* 189:40–53. DOI: 10.1111/j.1469-
533   8137.2010.03533.x.
534 Li QY, Qin Z, Jiang YM, Shen CC, Duan ZB, Niu JS. 2014. Screening wheat genotypes for
535   resistance to black point and the effects of diseased kernels on seed germination. *Journal of
536   Plant Diseases & Protection* 121:79–88. DOI: 10.1007/BF03356495.
537 Liao C, Zheng Y, Guo Y. 2017. MYB30 transcription factor regulates oxidative and heat stress
538   responses through ANNEXIN‐mediated cytosolic calcium signaling in Arabidopsis. *New
539   Phytologist* 216:163. DOI: 10.1111/nph.14679.
540 Liu L, Zou ZS, Qian K, Xia C, He Y, Zeng HL, Zhou X, Riemann M, Yin CX. 2017. Jasmonic
541   acid deficiency leads to scattered floret opening time in cytoplasmic male sterile rice
542   Zhenshan 97A. *Journal of Experimental Botany* 68:4613–4625. DOI: 10.1093/jxb/erx251.
543 Livak KJ, Schmittgen TD. 2001. Analysis of relative gene expression data using real-time
544   quantitative PCR and the 2-ΔΔCT Method. *Methods* 25:402–408. DOI:
545   10.1006/meth.2001.1262.
546 Lombardo F, Kuroki M, Yao SG, Shimizu H, Ikegaya T, Kimizu M, Ohmori S, Akiyama T,
547   Hayashi T, Yamaguchi T, Koike S, Yatou O, Yoshida H. 2017. The superwoman1-
548   cleistogamy 2 mutant is a novel resource for gene containment in rice. *Plant Biotechnology
549   Journal* 15:97–106. DOI: 10.1111/pbi.12594.
550 Ma J, Li R, Wang H, Li D, Wang X, Zhang Y, Zhen W, Duan H, Yan G, Li Y. 2017.
551   Transcriptomics Analyses Reveal Wheat Responses to Drought Stress during Reproductive
552   Stages under Field Conditions. *Front Plant Sci* 8:592. DOI: 10.3389/fpls.2017.00592.
553 Maeng JY, Won YJ, Piao R, Cho YI, Jiang W, Chin JH, Koh HJ. 2006. Molecular mapping of a
554   gene "ld(t)" controlling cleistogamy in rice. *Theoretical and Applied Genetics* 112:1429–
555   1433. DOI: 10.1007/s00122-006-0244-z.
556 Mortimer JC, Laohavisit A, Macpherson N, Webb A, Brownlee C, Battey NH, Davies JM. 2008.
557   Annexins: multifunctional components of growth and adaptation. *Journal of Experimental
558   Botany* 59:533. DOI: 10.1093/jxb/erm344.
559 Muqaddasi QH, Brassac J, Borner A, Pillen K, Roder MS. 2017. Genetic Architecture of Anther
560   Extrusion in Spring and Winter Wheat. *Front. Plant Sci* 8:754. DOI:
561   10.3389/fpls.2017.00754.
562 Nair SK, Wang N, Turuspekov Y, Pourkheirandish M, Sinsuwongwat S, Chen G, Sameri M,
563   Tagiri A, Honda I, Watanabe Y, Kanamori H, Wicker T, Stein N, Nagamura Y, Matsumoto
564   T, Komatsuda T. 2010. Cleistogamous flowering in barley arises from the suppression of

565   microRNA-guided HvAP2 mRNA cleavage. *Proceedings of the National Academy of*
566   *Sciences of the United States of America* 107:490–495. DOI: 10.1073/pnas.0909097107.
567 Ni DH, Li J, Duan YB, Yang YC, Wei PC, Xu RF, Li CR, Liang DD, Li H, Song FS, Ni JL, Li
568   L, Yang JB. 2014. Identification and utilization of cleistogamy gene cl7(t) in rice (Oryza
569   sativa L.). *J Exp Bot* 65:2107–2117. DOI: 10.1093/jxb/eru074.
570 Ning S, Wang N, Sakuma S, Pourkheirandish M, Wu J, Matsumoto T, Koba T, Komatsuda T.
571   2013. Structure, transcription and post-transcriptional regulation of the bread wheat
572   orthologs of the barley cleistogamy gene Cly1. *Theoretical and Applied Genetics* 126:1273–
573   1283. DOI: 10.1007/s00122-013-2052-6.
574 Ohmori S, Tabuchi H, Yatou O, Yoshida H. 2012. Agronomic traits and gene containment
575   capability of cleistogamous rice lines with the superwoman1-cleistogamy mutation. *Breed*
576   *Sci* 62:124–132. DOI: 10.1270/jsbbs.62.124.
577 Okada T, Jayasinghe J, Nansamba M, Baes M, Warner P, Kouidri A, Correia D, Nguyen V,
578   Whitford R, Baumann U. 2018. Unfertilized ovary pushes wheat flower open for cross-
579   pollination. *Journal of Experimental Botany* 69:399–412. DOI: 10.1093/jxb/erx410.
580 PARRY DW, JENKINSON P, McLEOD L. 1995. Fusarium ear blight (scab) in small grain
581   cereals—a review. *Plant Pathology* 44:207–238. DOI: doi:10.1111/j.1365-
582   3059.1995.tb02773.x.
583 Pissarek HP. 1971. Untersuchungen über Bau und Funktion der Gramineen-Lodiculae. *Beitrage*
584   *Zur Biologie Der Pflanzen* 47:313–370.
585 Poovaiah BW, Reddy ASN. 1993. Calcium and Signal-Transduction in Plants. *Critical Reviews*
586   *in Plant Sciences* 12:185–211. DOI: Doi 10.1080/713608046.
587 Pugh GW, Johann H, Dickson JG. 1933. Factors affecting infection of Wheat heads by
588   Gibberella saubiuetii. *J Agric Res* 46:771–797.
589 Qin Y, Yang J, Zhao J. 2005. Calcium changes and the response to methyl jasmonate in rice
590   lodicules during anthesis. *Protoplasma* 225:103–112. DOI: 10.1007/s00709-005-0086-6.
591 Rawat N, Pumphrey MO, Liu S, Zhang X, Tiwari VK, Ando K, Trick HN, Bockus WW,
592   Akhunov E, Anderson JA, Gill BS. 2016. Wheat Fhb1 encodes a chimeric lectin with
593   agglutinin domains and a pore-forming toxin-like domain conferring resistance to Fusarium
594   head blight. *Nat Genet* 48:1576–1580. DOI: 10.1038/ng.3706.
595 Sage GCM, De Isturiz MJ. 1974. The inheritance of anther extrusion in two spring wheat
596   varieties. *Theoretical and Applied Genetics* 45:126–133. DOI: 10.1007/bf00291142.
597 Schägger H. 2006. Tricine-SDS-PAGE. *Nature Protocols* 1:16–22. DOI: 10.1038/nprot.2006.4.
598 Scheltema RA, Hauschild JP, Lange O, Hornburg D, Denisov E, Damoc E, Kuehn A, Makarov
599   A, Mann M. 2014. The Q Exactive HF, a Benchtop Mass Spectrometer with a Pre-filter,
600   High-performance Quadrupole and an Ultra-high-field Orbitrap Analyzer. *Molecular &*
601   *Cellular Proteomics* 13:3698–3708. DOI: 10.1074/mcp.M114.043489.
602 Schroeder HW, Christensen JJ. 1963. Factors affecting resistance of Wheat to scab caused by
603   Gibberella zeae. *Phytopathology* 53:831.
604 Schuster R, Ellner FM. 2008. Level of Fusarium infection in wheat spikelets related to location
605   and number of inoculated spores. *Mycotoxin Research* 24:80–87. DOI:
606   10.1007/BF02985285.
607 Schweppe RE, Haydon CE, Lewis TS, Resing KA, Ahn NG. 2003. The characterization of
608   protein post-translational modifications by mass spectrometry. *Acc Chem Res* 36:453–461.
609   DOI: 10.1021/ar020143l.

610 Sharma M, Gupta SK, Majumder B, Maurya VK, Deeba F, Alam A, Pandey V. 2017. Salicylic
611   acid mediated growth, physiological and proteomic responses in two wheat varieties under
612   drought stress. *J Proteomics* 163:28–51. DOI: 10.1016/j.jprot.2017.05.011.
613 Turuspekov Y, Mano Y, Honda I, Kawada N, Watanabe Y, Komatsuda T. 2004. Identification
614   and mapping of cleistogamy genes in barley. *Theoretical and Applied Genetics* 109:480–
615   487. DOI: 10.1007/s00122-004-1673-1.
616 Untergasser A, Cutcutache I, Koressaar T, Ye J, Faircloth BC, Remm M, Rozen SG. 2012.
617   Primer3--new capabilities and interfaces. *Nucleic Acids Research* 40:e115. DOI:
618   10.1093/nar/gks596.
619 Unwin RD, Griffiths JR, Whetton AD. 2010. Simultaneous analysis of relative protein
620   expression levels across multiple samples using iTRAQ isobaric tags with 2D nano LC-
621   MS/MS. *Nature Protocols* 5:1574–1582. DOI: 10.1038/nprot.2010.123.
622 Vizcaino JA, Csordas A, del-Toro N, Dianes JA, Griss J, Lavidas I, Mayer G, Perez-Riverol Y,
623   Reisinger F, Ternent T, Xu QW, Wang R, Hermjakob H. 2016. 2016 update of the PRIDE
624   database and its related tools. *Nucleic Acids Research* 44:D447–D456. DOI:
625   10.1093/nar/gkv1145.
626 Walter S, Nicholson P, Doohan FM. 2010. Action and reaction of host and pathogen during
627   Fusarium head blight disease. *New Phytol* 185:54–66. DOI: 10.1111/j.1469-
628   8137.2009.03041.x.
629 Wang Z, Gu Y, Gao Y. 1991. Studies on the mechanism of the anthesis of rice III. structure of
630   the lodicule and changes of its contents during flowering. *Acta Agronomica Sinica* 17:96–
631   101.
632 Wang N, Ning S, Pourkheirandish M, Honda I, Komatsuda T. 2013. An alternative mechanism
633   for cleistogamy in barley. *Theoretical and Applied Genetics* 126:2753–2762. DOI:
634   10.1007/s00122-013-2169-7.
635 Wang N, Ning S, Wu J, Tagiri A, Komatsuda T. 2015. An epiallele at cly1 affects the expression
636   of floret closing (cleistogamy) in barley. *Genetics* 199:95–104. DOI:
637   10.1534/genetics.114.171652.
638 Winfield MO, Lu C, Wilson ID, Coghill JA, Edwards KJ. 2010. Plant responses to cold:
639   Transcriptome analysis of wheat. *Plant Biotechnol J* 8:749–771. DOI: 10.1111/j.1467-
640   7652.2010.00536.x.
641 Won YJ, Koh HJ. 1998. Inheritance of cleistogamy and its interrelationship between other
642   agronomic characters in rice. *Korean Journal of Breeding*.
643 Wu WW, Wang GH, Baek SJ, Shen RF. 2006. Comparative study of three proteomic
644   quantitative methods, DIGE, cICAT, and iTRAQ, using 2D gel- or LC-MALDI TOF/TOF.
645   *Journal of Proteome Research* 5:651–658. DOI: 10.1021/pr050405o.
646 Yan S, Tang Z, Su W, Sun W. 2005. Proteomic analysis of salt stress-responsive proteins in rice
647   root. *Proteomics* 5:235–244. DOI: 10.1002/pmic.200400853.
648 Yan H, Zhang B, Zhang Y, Chen X, Xiong H, Matsui T, Tian X. 2017. High Temperature
649   Induced Glume Closure Resulted in Lower Fertility in Hybrid Rice Seed Production. *Front*
650   *Plant Sci* 7:1960. DOI: 10.3389/fpls.2016.01960.
651 Yang Z, Guo GY, Zhang MY, Liu CY, Hu Q, Lam H, Cheng H, Xue Y, Li JY, Li N. 2013.
652   Stable Isotope Metabolic Labeling-based Quantitative Phosphoproteomic Analysis of
653   Arabidopsis Mutants Reveals Ethylene-regulated Time-dependent Phosphoproteins and
654   Putative Substrates of Constitutive Triple Response 1 Kinase. *Molecular & Cellular*
655   *Proteomics* 12:3559–3582. DOI: 10.1074/mcp.M113.031633.

656 Yang Z, Peng Z, Wei S, Liao M, Yu Y, Jang Z. 2015. Pistillody mutant reveals key insights into
657   stamen and pistil development in wheat (Triticum aestivum L.). *BMC Genomics* 16:211.
658   DOI: 10.1186/s12864-015-1453-0.
659 Yoshida H, Itoh J, Ohmori S, Miyoshi K, Horigome A, Uchida E, Kimizu M, Matsumura Y,
660   Kusaba M, Satoh H, Nagato Y. 2007. superwoman1-cleistogamy, a hopeful allele for gene
661   containment in GM rice. *Plant Biotechnol J* 5:835–846. DOI: 10.1111/j.1467-
662   7652.2007.00291.x.
663 Yoshida M, Kawada N, Tohnooka T. 2005. Effect of row type, flowering type and several other
664   spike characters on resistance to Fusarium head blight in barley. *Euphytica* 141:217–227.
665   DOI: 10.1007/s10681-005-7008-8.
666 Yumurtaci A, Sipahi H, Al-Abdallat A, Jighly A, Baum M. 2017. Construction of new EST-
667   SSRs for Fusarium resistant wheat breeding. *Comput Biol Chem* 68:22–28. DOI:
668   10.1016/j.compbiolchem.2017.02.003.
669 Zadoks JC, Chang TT, Konzak CF. 1974. A decimal code for the growth stages of cereals. *Weed*
670   *Research* 14:415–421.
671 Zange BJ, Kang Z, Buchenauer H. 2005. Effect of Folicur® on infection process of Fusarium
672   culmorum in wheat spikes / Wirkung von Folicur® auf den Infektionsprozess von Fusarium
673   culmorum in Weizenähren. *Zeitschrift Für Pflanzenkrankheiten Und Pflanzenschutz*
674   112:52–64.
675 Zee S, O'Brien T. 1971. The Vascular Tissue of the Lodicules of Wheat. *Australian Journal of*
676   *Biological Sciences* 24:797–804.
677 Zhang X, Guo B, Lan G, Li H, Lin S, Ma J, Lv C, Xu R. 2016. A Major QTL, Which Is Co-
678   located with cly1, and Two Minor QTLs Are Associated with Glume Opening Angle in
679   Barley (Hordeum vulgare L.). *Front. Plant Sci* 7:1585. DOI: 10.3389/fpls.2016.01585.
680 Zhang H, Han B, Wang T, Chen S, Li H, Zhang Y, Dai S. 2012. Mechanisms of plant salt
681   response: insights from proteomics. *J Proteome Res* 11:49–67. DOI: 10.1021/pr200861w.
682 Zhao Q, Zhang H, Wang T, Chen S, Dai S. 2013. Proteomics-based investigation of salt-
683   responsive mechanisms in plant roots. *J Proteomics* 82:230–253. DOI:
684   10.1016/j.jprot.2013.01.024.
685
686
687

Figure 1

Figure 1. Characteristics of genotypes in the 2 differential individual lines of YM18 and *ZK001*.

Figure 1. Characteristics of genotypes in the 2 differential individual lines of YM18 and *ZK001*. A: Comparison of the inflorescence details between YM18 and *ZK001* in post-anthesis stage (Bar = 1 cm) (A). B: Lodicules of YM18 (B) and *ZK001* (C) which were sampled in GAS and cultured on MS media containing graphite were ovserved after 90 minutes by microscope (Bar = 1 mm).
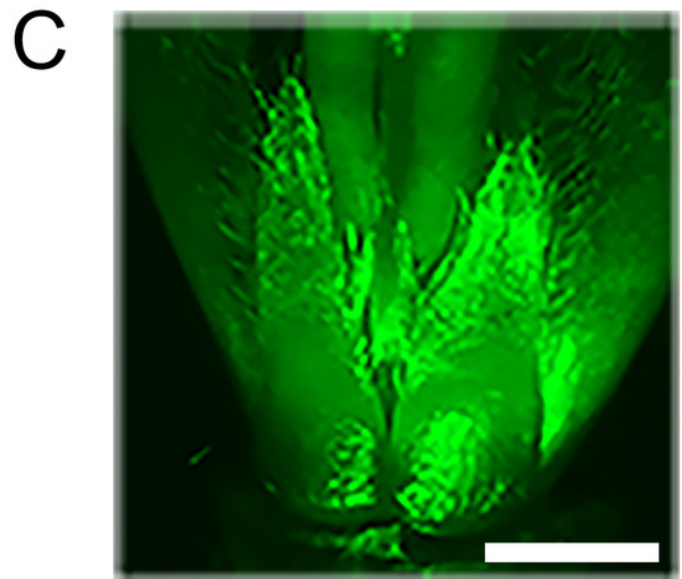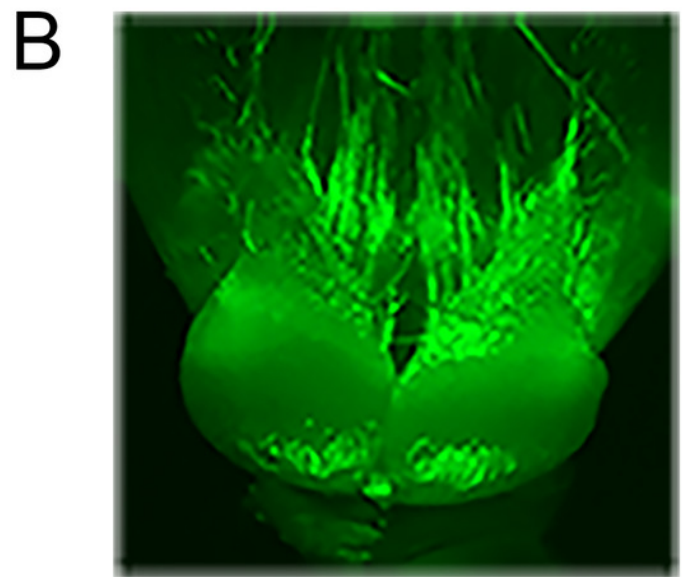
Figure 2

Figure 2. Starch, soluble sugar content in lodicules of YM18 (green line) and *ZK001* (red line).

Figure 2. Starch, soluble sugar content in lodicules of YM18 (green line) and *ZK001* (red line). **A** and **B:** comparison of starch content change tendency in lodicules between YM18 and *ZK001*. **C** and **D:** comparison of soluble sugar content change tendency in lodicules between YM18 and *ZK001*. PL[1]: pair of lodicules (PL). The results presented are the means of three independent experiments. Error bars, s.d.
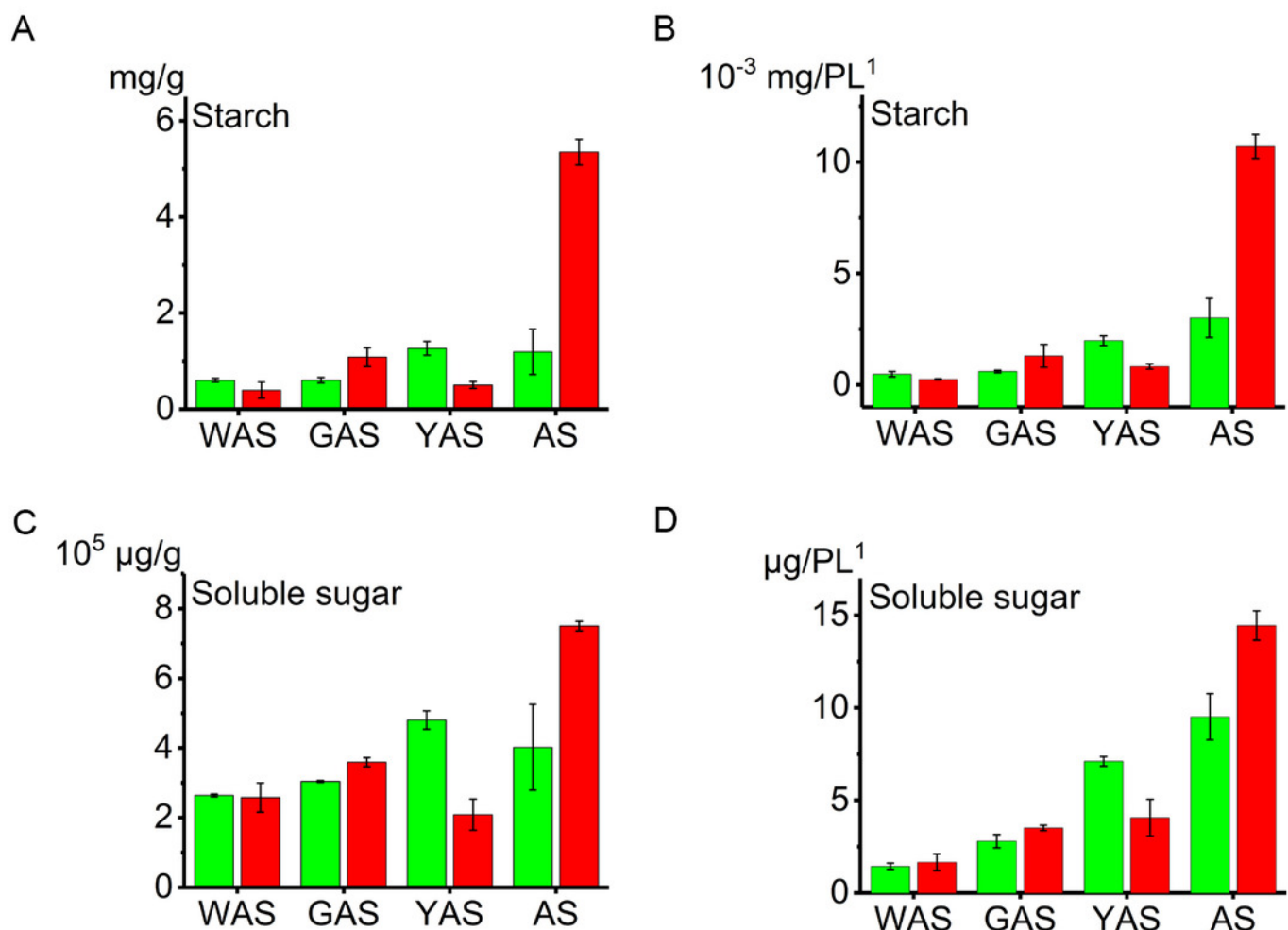
Figure 3

Figure 3. Assessment of iTRAQ analysis for peptides identification and quantitation.

Figure 3. Assessment of iTRAQ analysis for peptides identification and quantitation. **A**: The distribution of the identification peptide segments counts corresponding to the identification of proteins number. **B**: Distribution of protein's molecular weight. **C**: Quantification of peptide-length coverage in the identified proteins. **D**: Coverage of protein mass distribution.
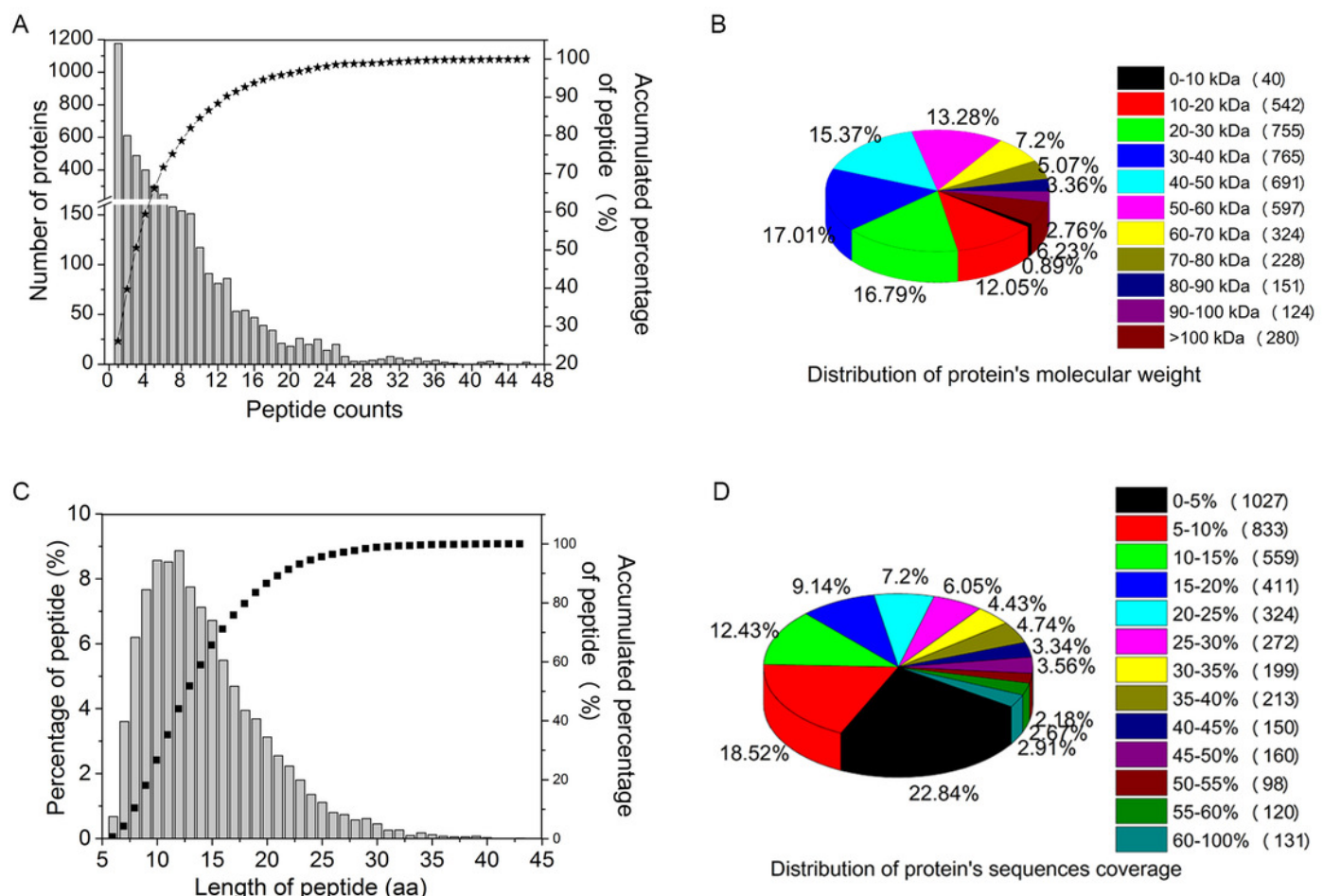
Figure 4

Figure 4. GO classification of DEPs of Group 1 to 4 from four flower development stages in YM18 and ZK001 based on GO enrichment.

Figure 4. GO classification of DEPs of Group 1 to 4 from four flower development stages in YM18 and ZK001 based on GO enrichment. **A**: molecular function of Group 1; **B**: biological process of Group 1; **C**: biological process, cellular component and molecular function of Group 2. No protein was enriched in Group 3 or Group 4 basing on GO enrichment. (0.667 < FC < 1.5, corrected P–value < 0.01, PSMs ≥ 2)
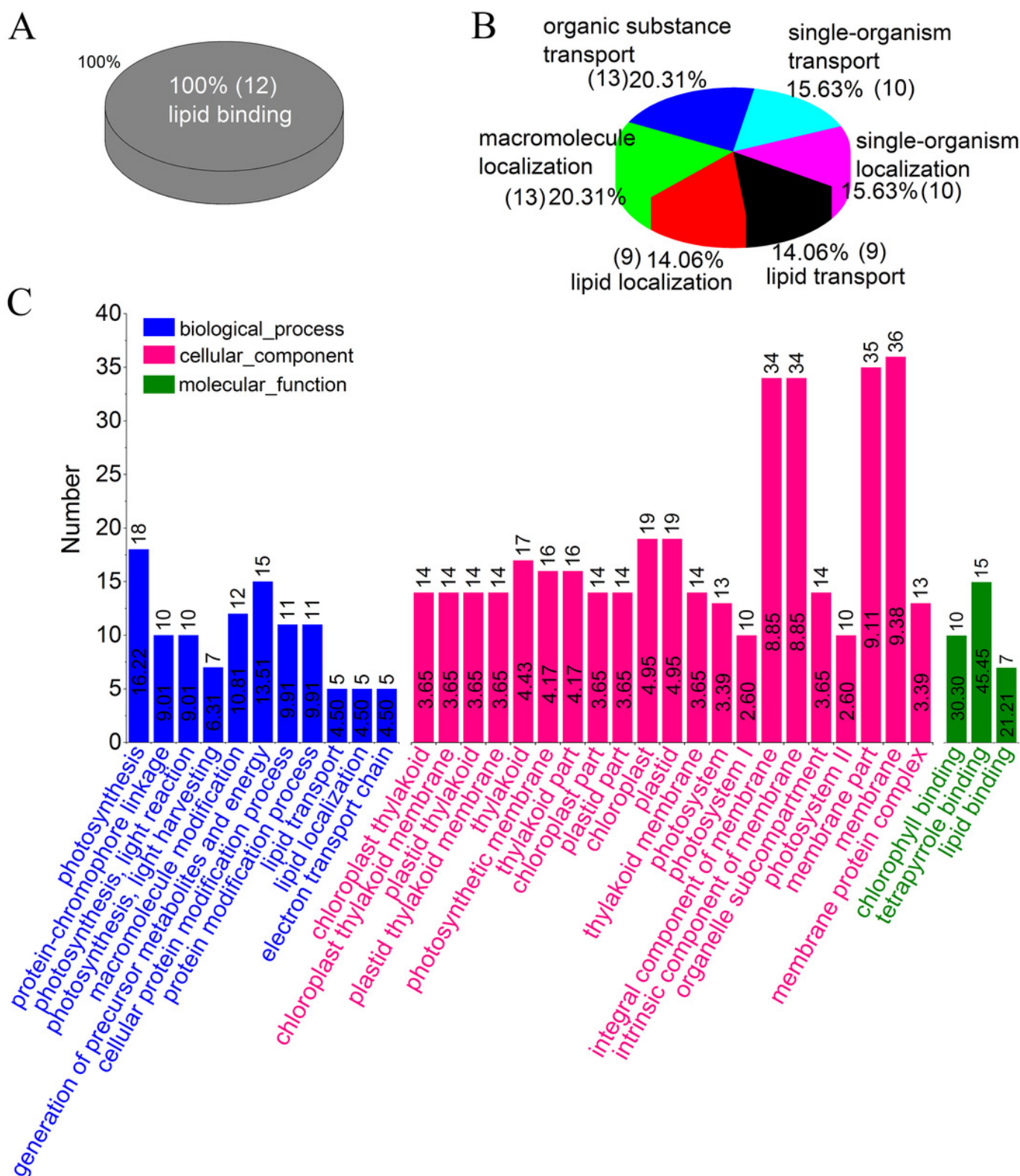
Figure 5

Figure 5. Relative expression profile of related genes which corresponded to DEPs in lodicules of YM18 (green column) and *ZK001* (red column).

Figure 5. Relative expression profile of related genes which corresponded to DEPs in lodicules of YM18 (green column) and *ZK001* (red column). **A to I:** relative expression profile of carbohydrate-related genes in lodicules of YM18 and *ZK001*. **J to K:** relative expression profile of calcium ion binding-related genes in lodicules of YM18 and *ZK001*. The results presented are the means of three independent experiments. Error bars, s.d. Columns marked with different lowercase letter indicate difference in means using the one-way ANOVA LSD analysis of PASW Statistics software. Duncan tests (*P* < 0.05) were used to detect significant differences between means.
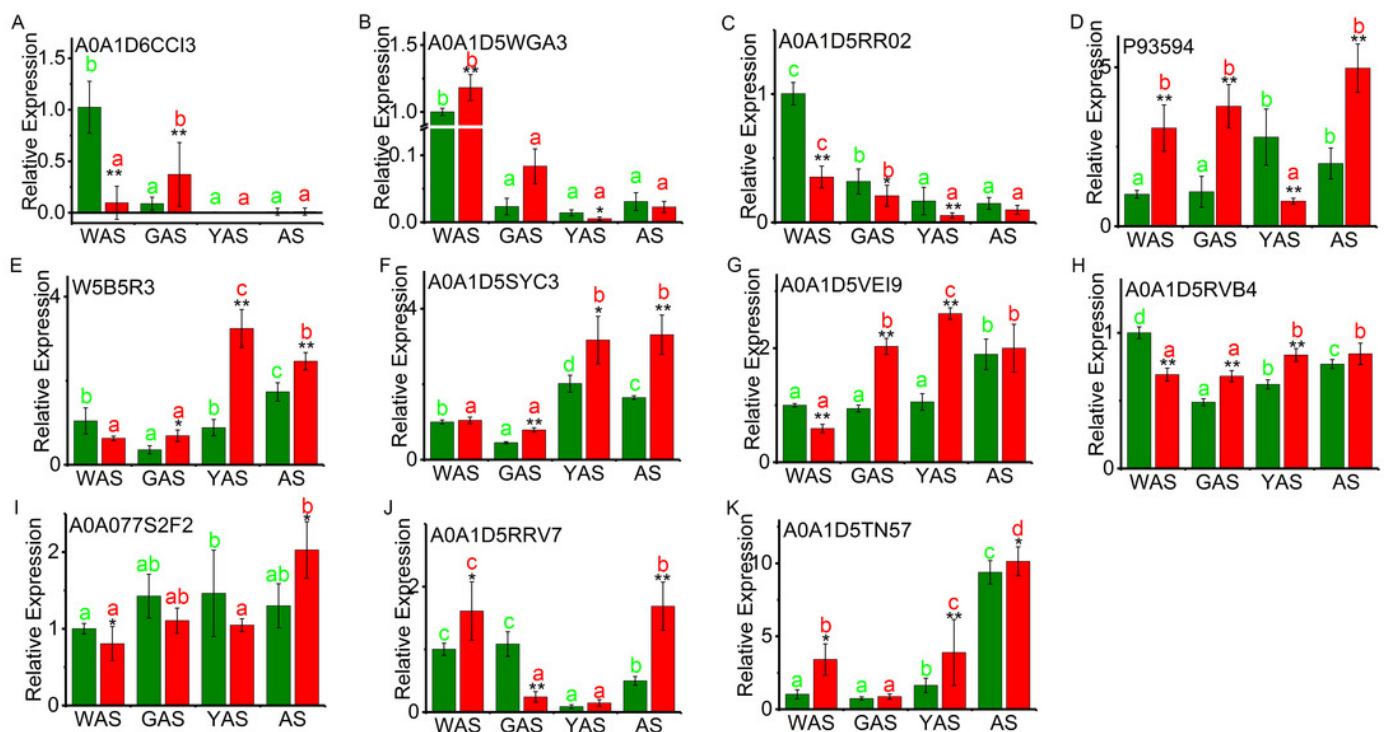
Figure 6

Figure 6. An overview of the pathway for proteome metabolic changes between YM18 and *ZK001*.

Figure 6. An overview of the pathway for proteome metabolic changes between YM18 and *ZK001*.
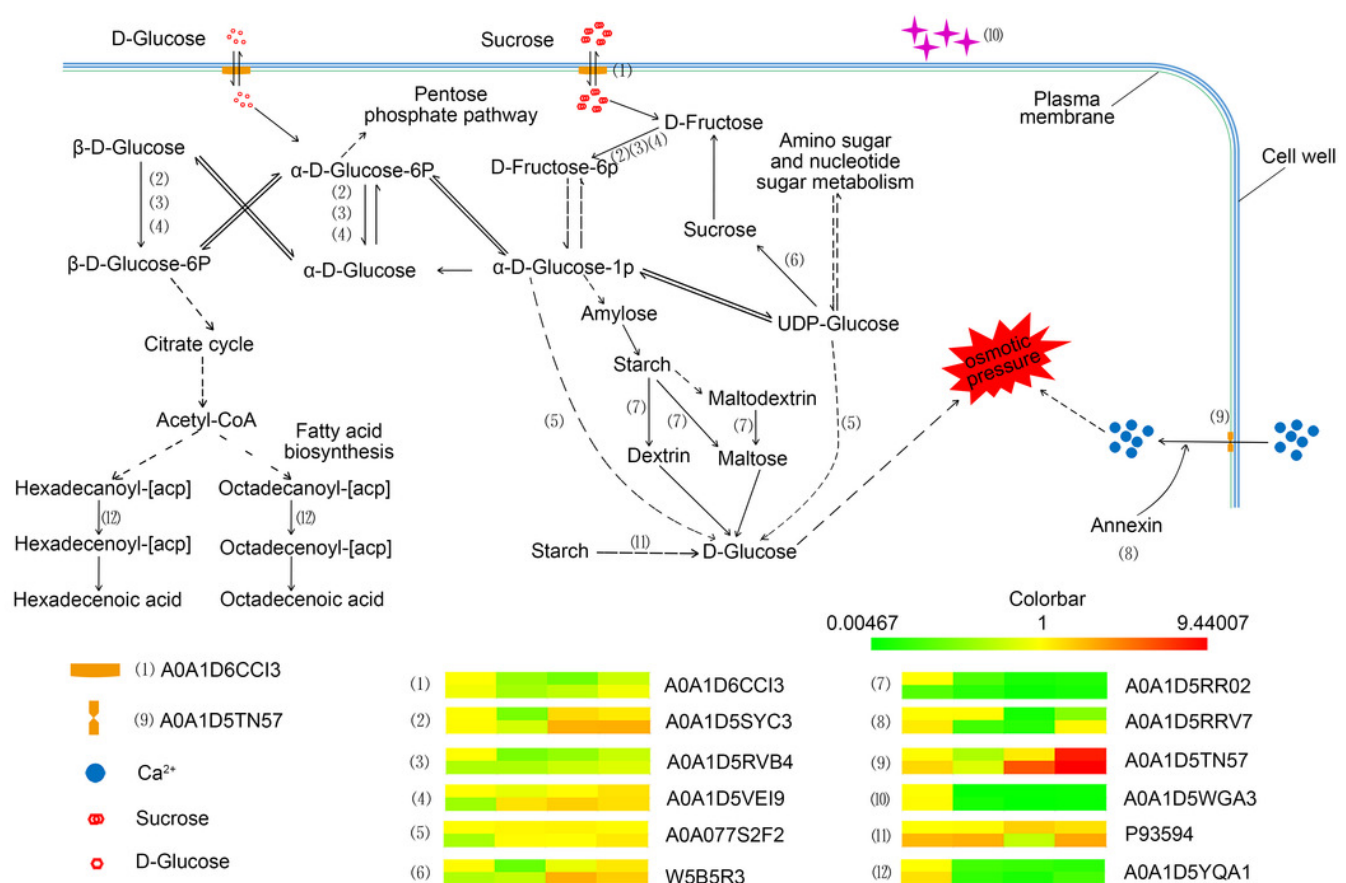
Table 1 Infection type produced by adult plant stage's material tested in 2014 and 2015.

Table 1 Infection type produced by adult plant stage's material tested in 2014 and 2015.

1   **Table 1**. Infection type produced by adult plant stage's material tested in 2014 and 2015.

Species	Diseased spikelets rate[a] (%)	
	2013-2014	2014-2015
SM3	7.03 ± 2.23	8.61 ± 3.40
ZK001	9.39 ± 3.31	17.60 ± 3.60
YM18	15.20 ± 2.46	35.16 ± 3.71
AK58	20.41 ± 6.76	38.12 ± 6.13

2   a: Diseased spikelets rate=the number of infected spikelets/total number of spikelets×100. The results presented are

3   the means of three independent experiments. Error bars, s.d.

Table 2. The number of differentially expressed proteins at four flower development stages.

Table 2. The number of differentially expressed proteins at four flower development stages.

(0.667 < FC < 1.5, corrected P–value < 0.01)

1   **Table 2**. The number of differentially expressed proteins at four flower development stages. (0.667 < FC < 1.5,

2   corrected P–value < 0.01, PSMs ⩾ 2)

Groups	Total	Corrected P–value < 0.01		
		Up-DEPs	Down-DEPs	Total DEPs
Group 1	4188	7	9	16
Group 2	4188	9	38	47
Group 3	4189	1	1	2
Group 4	4189	0	0	0
Group 5	4188	0	11	11
Group 6	4188	27	97	124
Group 7	4188	31	74	105
Group 8	4188	4	11	15
Group 9	4188	123	175	298
Group 10	4188	94	94	188